



Comparative Analysis of Wavelet bi-spectrum and Power Spectrum Features for the Classification of Adventitious Lung Sound

Rupesh Dubey^{1,2}, Rajesh M. Bodade³ and Divya Dubey⁴

¹Associate Professor, Department of Electronics and Communication Engineering, Indore (Madhya Pradesh), India.

²Research Scholar, Military College of Telecomm. Engineering (MCTE), MHOW, Ministry of Defense, Government of India, DAVV University, Indore (Madhya Pradesh), India.

³Professor, Military College of Telecommunication Engineering (MCTE), MHOW, Ministry of Defense, Government of India, Indore (Madhya Pradesh), India.

⁴Assistant Professor, Department of Electronics and Communication Engineering, SDBCE Indore (Madhya Pradesh), India.

(Corresponding author: Rupesh Dubey)

(Received 15 January 2020, Revised 14 April 2020, Accepted 15 April 2020)

(Published by Research Trend, Website: www.researchtrend.net)

ABSTRACT: Lung sounds convey essential information about the health of the patient. Accurate detection, followed by the analysis of adventitious sounds, is still a significant challenge. Suitable techniques for the same shall empower to deal with the problem of scarcity of expert physicians. The conventional techniques suffer from the identification of suitable features that can provide higher accuracies of detection. Here features based on higher-order spectral for wavelet bi-spectrum (WBS) and Power Spectrum (PS) are introduced and analyzed for the classification of adventitious sounds of lungs, namely wheezes, crackle, and normal sound. Comparison is presented between higher-order spectral features based on wavelet bi-spectrum and power spectrum using classifiers like decision tree, SVM, k-NN, ensemble learner. Here results of accuracy are explored for the feature and sub classifier combination. Many feature classifier combination has yielded accuracy as high as 100%. Average accuracy achieved in the case of wavelet bi-spectrum outperforms that achieved for features based on the power spectrum.

Keywords: Higher-order spectral, k-NN, SVM, classification tree, wheezes, crackle.

Abbreviations: Global Peak GP, Local Peak LP, Support Vector Machine SVM, k-Nearest Neighbor k-NN, A- Asthma, Acy. Accuracy, AWS- Available with Source, BPF- Band Pass Filter, Bu.- Butter Worth C-Crackle, CA-Commercially Available, CAcc. Contact Accelerometer, CC- Coarse Crackle, DT- Decision Tree, DR- Dry rale, DS- Digital Stethoscope, EL- Ensemble Learner, ES- Electronics Stethoscope, Fpr- Friction pleural rub, HLS-Healthy Lung Sound, HPF- High Pass Filter, Lab. – Laboratory, LPF- Low Pass Filter, MR- Moist rale, N-Subjects/Signals, NA- Not Available, NM- Not Mentioned, NU- Not Used O- Order, S-Sensitivity, SF- Sampling Frequency, So- Stridor, SP- Specificity, SR- Sampling Rate, W- Wheeze, WCC- Wavelet Packet Transform, WBP-Wavelet bi-phase, WBS-Wavelet bi-spectrum, Yrs.- Years.

I. INTRODUCTION

As per WHO [1], over 80% of death in the case of obstructive pulmonary diseases like Asthma and Chronic Obstructive Pulmonary Diseases (COPD) occurs in low and lower-middle-income countries. Adventitious sounds like wheezes and crackle are heard during breathing cycles of patients suffering from obstructive pulmonary diseases [2]. Wheezes have a time length greater than 150 ms, whereas for crackle, it less than 20 ms [2]. Wheezes exhibit continuous waveform, while for crackle, the waveforms are discontinuous. Experienced human ears can easily recognize adventitious sounds. The traditional stethoscope was invented in the year 1821. These suffer limitations of lower frequency (<120Hz). Previous signal processing techniques for the identification of wheezes were based on time-expanded waveforms [3]. Further works followed to focus on peaks detection in the spectrum, their amplitude, and pitch range [4, 5]. Researchers employed various classification techniques for the labeling of features like neural networks [6].

Shi *et al.*, (2019) also used BPNN as a classification method with the WCC feature but achieved 92.5% accuracy [7]. CNN, which was initially introduced for image processing, is being employed for lung sound analysis with a lower number of data set achieved 97% accuracy [8]. The accuracy of algorithms that are based on the above criteria depends upon the acoustics amplitude of the signals. There remains a need to focus on techniques independent of amplitudes, so that accuracy of detection remains unaffected by location and device of sound capture. The obstruction in airways results in changes in non-linear harmonic peaks interaction. They have non-stationary characteristics; contain non-linearity in their harmonic interactions. Wheezes show a phase relationship with quadratic phase coupling. Some researchers have employed bi-coherence [9] and phase spacing features for the analysis of lung sound [10]. Also, works are clubbing continuous wavelet transform with third-order spectra [11]. The severity of asthma is also identified in some of the approaches by using integrated power [12].

Taplidou and Hadjileontiadis (2010) have used higher-order spectral features for the classification of adventitious sounds. Accuracy of detection (96%) is calculated using statistical properties (SPSS tool). The research used a significant number of features and achieved lower accuracy of detection [13].

The feature abbreviation rules, as introduced in the research [13], are followed in this paper with the addition of the rules for the features based on the power spectrum.

Here for the identification of nonlinearity in adventitious sound wavelet bi-spectrum and power spectrum features are employed. A comparative analysis of the accuracy of detection is presented between features based on the wavelet bi-spectrum and power spectrum.

The rest of the paper is organized as section II discusses the mathematics bases related to features, section III presents data analysis, section IV put light on validation approaches. section V explains classification methods followed in the research, section VI presents the experimental results finally section VII concludes the paper.

II. MATHEMATICAL BASIS AND FEATURE SET

Conditions of signal capture from lung and the capturing devices are not standardized, so signal detection by features based on their amplitudes is a challenging task. There is an urgent necessity to introduce features independent of signal amplitude. The higher-order features target the nonlinear and non-Gaussian parameters of the signal. The bi-spectrum estimation extracts the degree of quadratic phase coupling between frequency components.

A. Wavelet bi-spectrum (WBS)

For the transient properties of the signal, the signal is convolved with wave-like structures (wavelets). The continuous wavelet transform defined as follows [14]

$$W_x(a, b) = \frac{1}{\sqrt{a}} \int_{-\infty}^{+\infty} x(t) \psi^* \left(\frac{t-b}{a} \right) dt \quad (1)$$

here, $x(t)$ is the signal in time-domain ($x(t) \in L^2(\mathbb{R})$), $*$ represents complex conjugate, and $\psi(t)$ signifies the mother wavelet with a as scaling and b as dilation factor, and both are continuous. The combination of bi-spectrum with the wavelet is called wavelet bi-spectrum. Here along with continuous wavelet transform, time-frequency is preferred. Wavelet type complex Morlet is selected [11, 14].

$$\psi(t) = \frac{1}{\sqrt{\pi f_b}} e^{-t^2 / f_b} e^{j2\pi f_c t} \quad (2)$$

here, f_c is the central wavelet frequency, and f_b is the bandwidth parameter.

The WBS is defined as [15] [16]

$$WB_x(a_1, a_2) = \int_T W_x^*(a, \tau) W_x(a_1, \tau) W_x(a_2, \tau) d\tau \quad (3)$$

The integration is done over a finite interval of time $T: \tau_0 \leq \tau \leq \tau_1$ and a , a_1 , and a_2 are the scale length of wavelet components and signal, respectively.

B. Power spectrum

The power spectrum can be calculated with less computational cost by the Welch method [17]. In this method, there are options to select the type, width, and amount of overlap of a window. The window type here is Kaiser window with a 50% overlap. The window width is such that the frequency resolution of the Welch spectrum is equal to the average dB in the width of the DFT spectrum.

If $X(j)$, $j=0, \dots, N-1$ be the samples from second-order stochastic sequence here, $E(x)=0$ and $P(f)$ is spectral density, if $|f| \leq \frac{1}{2}$

The segments overlap of length L with D units apart, and the K_{th} segment is defined as

$$\begin{aligned} X_1(j) &= X(j) \quad j=0, \dots, L-1 \\ X_2(j) &= X(j+D) \quad j=0, \dots, L-1 \end{aligned} \quad (4)$$

Finally

$$X_k(j) = X(j+(K-1)D) \quad j=0, \dots, L-1 \quad (5)$$

here $N=(K-1)D+L$ segments are as shown in Fig. 1.

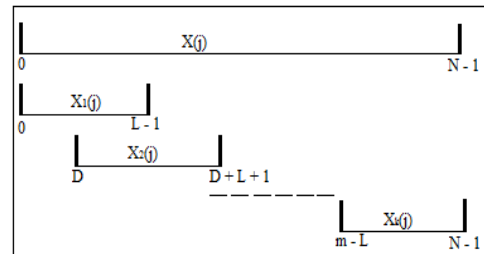


Fig. 1. Segment division of signal.

For each segment of Length L , modified periodogram is calculated

$X_k(j) W(j), \dots, X_k(j) W(j)$, here $W(j)$ is data window, $j=0, \dots, L-1$, now take FFT

$$A_k(n) = \frac{1}{L} \sum_{j=0}^{L-1} X_k(j) W(j) e^{-2\pi i j n / L} \quad \text{and } i=(-1)^{1/2} \quad (6)$$

$$I_k(f_n) = \frac{L}{U} |A_k(n)|^2 \quad k = 1, 2, \dots, K, \quad \text{here } f_n = n/L \quad (7)$$

$$U = \frac{1}{L} \sum_{j=0}^{L-1} W^2(j) \quad (8)$$

Spectral estimation is the average of this periodogram

$$\hat{P}(f_n) = \frac{1}{K} \sum_{k=1}^K I_k(f_n) \quad (9)$$

C. Feature set

Here features under consideration are nonlinear in the time-frequency domain, and they are related to nonlinear and non-stationary signal characteristics. The characteristics of the signal appear in the quadratic phase coupling of distinct harmonic peaks and their appearance over time. Figs. 2 to 7 gives a view of the wavelet bi-spectrum and power spectrum obtained for different adventitious sounds. The figures give the scope of availability of a rich feature base.

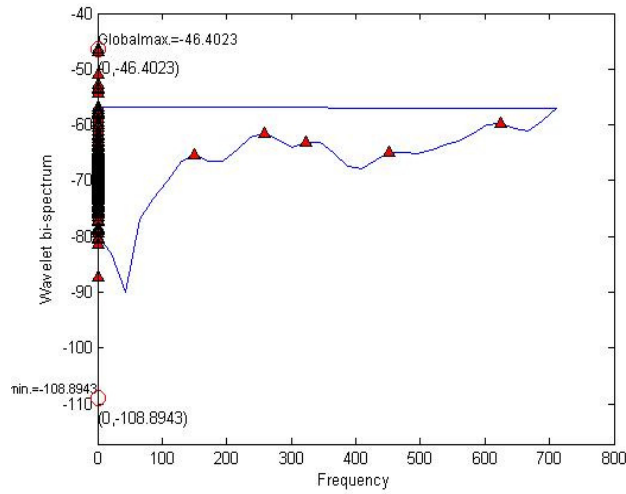


Fig. 2. Wavelet bi-spectrum feature of the wheeze.

Table 1: List of features and their abbreviations.

Feature	Feature description	Abbreviation
1	Global max value in the amplitude domain in wavelet bi-spectrum	$G_{Max}WB_x$
2	Global min value in the amplitude domain in wavelet bi-spectrum	$G_{Min}WB_x$
3	The distance of the C_i from the contour S of the i_{th} GP at the bi-frequency domain in wavelet bi-spectrum	$D^{GPI}WB_x$
4	Amplitude above mean in wavelet bi-spectrum	$A_{mean}WB_x$
5	Mean wavelet bi-spectrum related to LPs	$meanWB_x^{LP}$
6	Average instantaneous wavelet bi-spectrum across the examined total time interval T	$mWB_x(\omega_1, \omega_2)$
7	Maximum wavelet bi-spectrum across time-related to LPs	$maxWB_x^{LP}$
8	The standard deviation of the wavelet bi-spectrum related to LPs	$stdWB_x^{LP}$
9	Global max value in the amplitude domain in the power spectrum	$G_{Max}P_x$
10	Global min value in the amplitude domain in the power spectrum	$G_{Min}P_x$
11	The distance of the C_i from the contour S of the i_{th} GP at the bi-frequency domain in the power spectrum	$D^{GPI}P_x$
12	Amplitude above mean in the power spectrum	$A_{mean}P_x$
13	Mean power spectrum related to LPs	$meanP_x^{LP}$
14	Average instantaneous Power spectrum across the examined total time interval T	$mP_x(\omega_1, \omega_2)$
15	Maximum power spectrum across time-related to LPs	$maxP_x^{LP}$
16	The standard deviation of the power spectrum related to LPs	$stdP_x^{LP}$

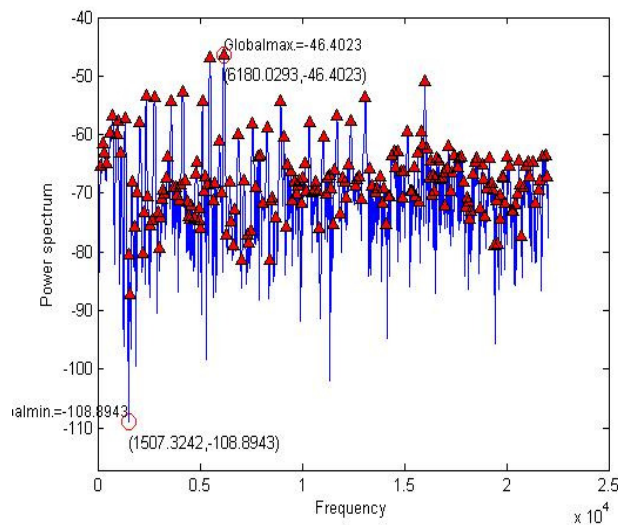


Fig. 3. Power spectrum feature of wheeze.

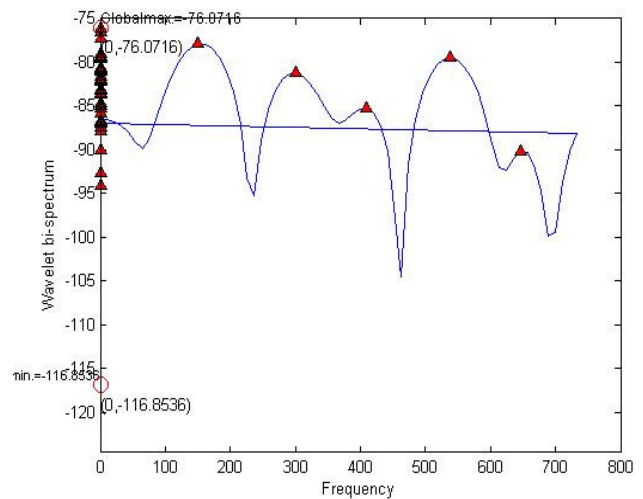


Fig. 4. Wavelet bi-spectrum feature of crackle.

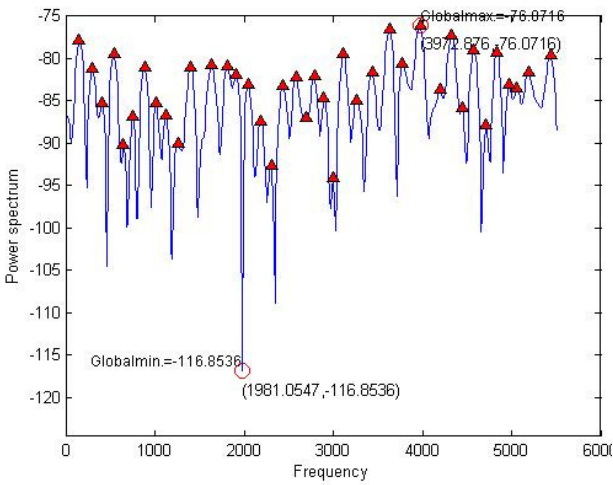


Fig. 5. Power spectrum feature of crackle.

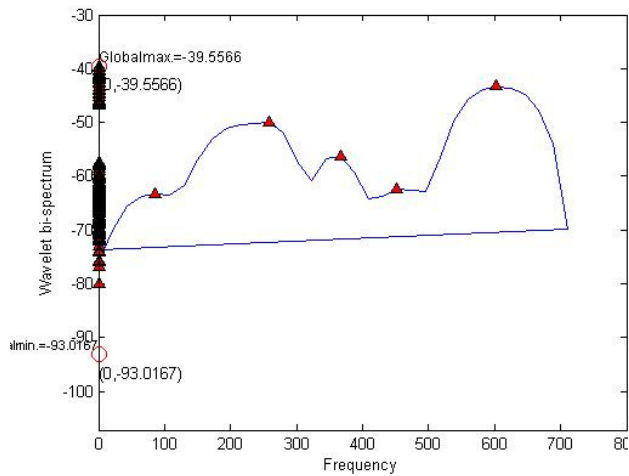


Fig. 6. Wavelet bi-spectrum feature of normal sound.

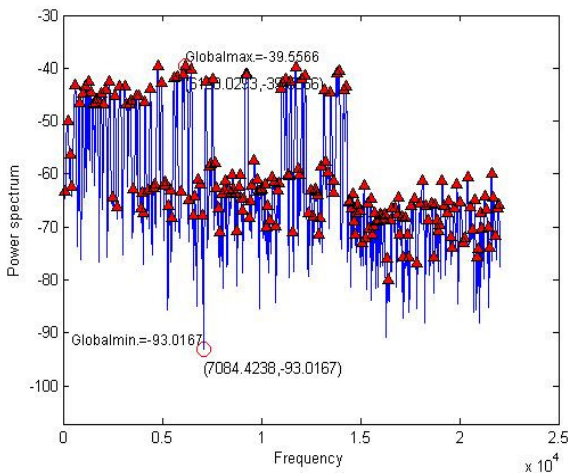


Fig. 7. Power spectrum feature of normal sound.

D. Global Peaks (GPs)

Peaks identified considering signal for full time duration, i.e., defined over $T=T_{Total}$, are referred to as Global

Peaks (GPs). Their different characteristics provide wavelet bi-spectrum and power spectrum-related characteristics of the proposed feature. The peak is identified as GP if its amplitude is higher than the mean of the average amplitude of peaks. Computation time is reduced by averaging instantaneous wavelet bi-amplitude across the whole time interval T , stationary in the bi-frequency domain.

$$mA_x(\omega_1, \omega_2) = A_x(\omega_1, \omega_2, t) \quad (10)$$

Here, $A_x(\omega_1, \omega_2, t)$ is the IWBC amplitude of instantaneous wavelet bi-amplitude over the area Δ exceeding statistical noise [11, 18].

$$mAb_x^{GP_i}(\omega_{c1}, \omega_{c2}) = mAb_x^{GP_i}(\omega_1, \omega_2) \Big|_{mA_x^{GP_i}(\omega_1, \omega_2)=\max} \quad (11)$$

$$C^i = (\omega_{c1}, \omega_{c2}), i = 1, 2, \dots, I$$

E. Local Peaks (LPs)

These are the peaks that are seen in the detailed perspective span of the signal based on window overlapping sections Δ obtained by using IWBS analysis. The appearing peaks are designated as Local Peaks (LPs).

$$Ab_x^{LP_i}(\omega_{c1}, \omega_{c2}, t) = Ab_x^{LP_i}(\omega_1, \omega_2, t) \Big|_{mA_x^{LP_i}(\omega_1, \omega_2, t)=\max} \quad (12)$$

Here, I is the number of LPs and i being the position of maximum peak.

III. DATA ANALYSIS

Data from different means have been used for the analysis of the algorithm. The R.A.L.E.[®] (Respiration Acoustics Laboratory Environment) Lung Sounds 3.2 [19] and other Internet resources [20-22]. Program for education and learning R.A.L.E.[®] lung sound is designed for doctors, educators, students, nurses, and health professionals. Respiratory acoustician laboratory of the University of Manitoba Winnipeg, Canada, runs the program. It has more than 50 respiratory sounds recording collections, of various age groups and diseases. Quiz section contributes an additional 24 cases. The collection is felicitated by awarded the Merit of computer-based materials by Health Sciences Communications Association. The data comprise of wheezes (normal, mono, and polyphonic) 252, crackle (coarse and fine) 70, normal sound (bronchial, tracheal, and bronchovesicular sounds) 50.

A. Data pre-processing

Sound signal sampling is done at 4 kHz, 16 bits with 1024 points per segment with the range -5.0V to +5.0V (-32,767 to +32,768). As per the Computerized Respiratory Sound Analysis (CORSA) guidelines, first-order Butterworth filter is used for high pass signals at 7.5 Hz to filter out DC offsets. Low pass filtration is done at 2.5 kHz by using eighth order Butterworth L.P.F., also, B.P.F. is done (150 Hz~2 kHz) for heart sound cancellation. The Goldwave[®] software is used to divide the signal into segments of their waveform. A pulmonologist performed manual validation of the database in the medical clinic at Indore, India.

IV. k-FOLD CROSS-VALIDATION APPROACH

Cross-validation is one of the commonly used method as a robust model for selection. The method with some

prior assumptions is rarely tied to a particular feature of an algorithm.

Cross-validation aims to estimate the performance of the learned model from data using an algorithm. The cross-validation can be used to estimate the generalization of an algorithm or to compare the performance of two or more different algorithms.

The conventional k-fold cross-validation follows:

D= Training set

k= Number of a fold (k=10)

C= Selected Classifier

– Divide D into k folds

– Model-based on C using k-1 folds

– Test the model in step 2 using the k fold.

– Repeat step 3 for every fold [23].

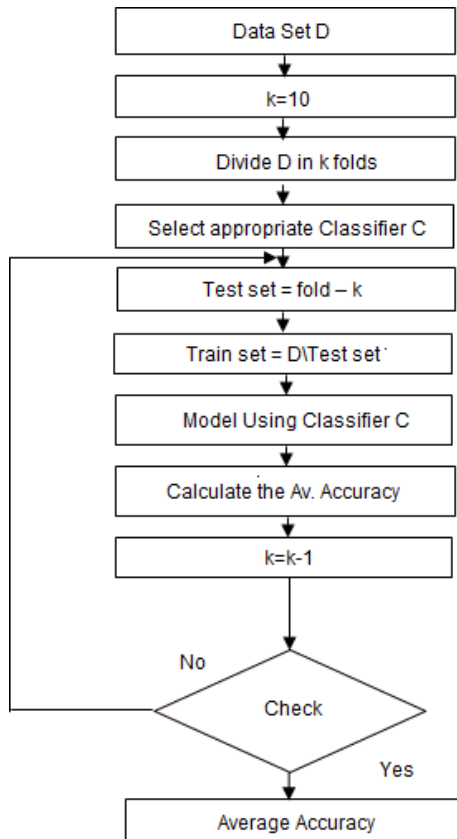


Fig. 8. Flow chart of the cross-validation method.

V. CLASSIFICATION METHODS

There are four classification methods employed in this research. Each method has three to six sub classifiers, as shown in Fig. 9.

A. Decision Tree [24]

They fall into the category of non-parametric supervised learning methods. The tree structure has two types of nodes, leaf and internal nodes. The majority vote of training examples reaching that leaf designates the class label. Internal nodes branch out according to answers. The splits are non-leaf nodes and are associated with feature tests.

In the case of the coarse tree, the slit is kept as 100. The medium tree uses fewer leaves than a fine tree. In

fine tree coarse distinctions between clauses are achieved using a lesser number of leaves.

The result is obtained when a leaf node is approached after the conduction of a series of feature tests. In each step, a data set is identified, and a split is selected, then this split is used to divide the data set into subsets, and each subgroup remains data set for the next step.

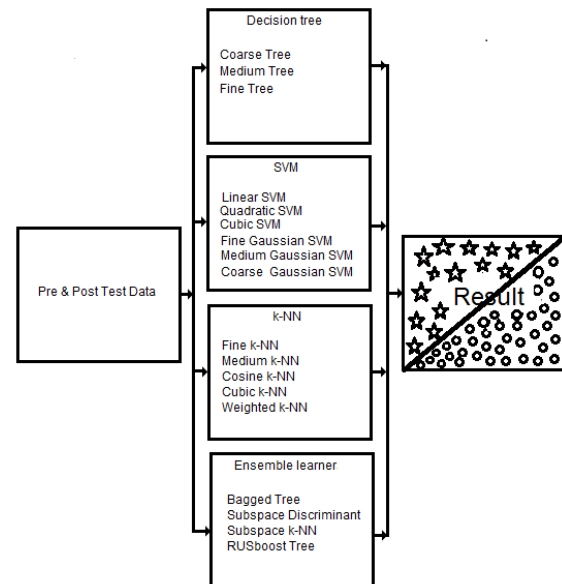


Fig. 9. Supervised classification approaches.

B. Support Vector Machine (SVM) [25, 26]

SVM is one of the most effective supervised classification algorithms. With a set of training examples and marked categories, SVM training builds a model that assigns new cases to one type or the other. SVM is mostly used as a non-probabilistic classification method. Linear SVM uses a linear kernel similarly cubic and quadratic SVM uses cubic and quadratic kernel, respectively. Fine, medium, and Gaussian SVM uses a Gaussian kernel with a kernel scale. It is finely detailed and less finely and mid-class between the two, respectively.

C. k-Nearest Neighbor Classifier [27]

Here, specifying the number of nearest neighbors provides the decision of the classification process. It is a non-parametric learning algorithm, which means, here all or most of the training data is employed during the testing phase.

Number k makes a circle, and the class or label of an unknown feature is assigned based on the largest number count of a particular class among all classes in that circle.

D. Ensemble Learner [28]

In this method, the decision to label a class is achieved by combining the decisions of the individual classifiers. In ensemble learners bagging and boosting classifiers are most widely used.

In the Bagging tree, an additional data set is generated from the original data set to achieve a decrease in the variance of prediction. Boosting involves a two-step approach. In the first step, subsets of the original data are obtained to achieve a series of averagely

performing models. In the second step, to achieve an increase in performance, a voting scheme is used to club the previous performances together.

VI. RESULTS

Here adventitious sounds are classified by a total of 16 (equally divided among both categories) features based on WBS and PS. There are in total 36 results presented for the set of feature sub classifier combinations. As summarized in Table 2, accuracy as high as 100% is obtained in the feature sub classifier combination like fine k-NN, weighted k-NN for both types of features, bagged tree, and subspace k-NN with power spectrum feature. Also, the highest accuracy is achieved in the case of RUSboost Tree with WBS feature using Matlab[®] 2019b. Parallel coordinate graphs (Fig. 10-13) are used for the analysis of multi-variable data and visualization of high-dimensional geometry. These have n parallel lines, typically erected vertical and spaced equally.

Predictions: model 2.1 (Linear SVM)

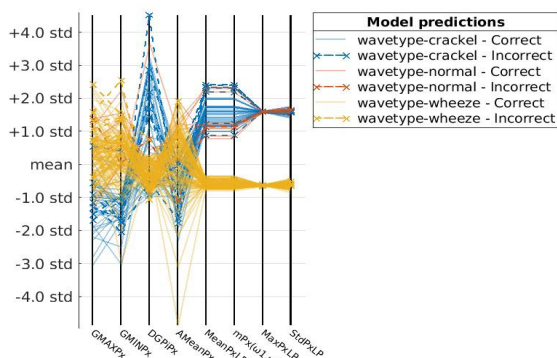


Fig. 10. Parallel coordinates graph of linear SVM in wavelet bi-spectrum.

Table 2: Summary of the accuracy of detection chart obtained in different classifier feature combination.

Data mining Technique	Classifier Type	Accuracy of WBS (%)	Accuracy of PS(%)
Decision tree	Coarse Tree	92.5	93.3
	Medium Tree	99.2	98.9
	Fine Tree	99.2	98.9
SVM	Linear SVM	94.1	91.9
	Quadratic SVM	95.2	94.4
	Cubic SVM	94.6	95.2
	Fine Gaussian SVM	96.5	97.8
	Medium Gaussian SVM	95.2	94.9
	Coarse Gaussian SVM	90.6	91.4
k-NN	Fine k-NN	100	100
	Medium k-NN	93.5	92.2
	Cosine k-NN	93.0	93.0
	Cubic k-NN	93.0	91.7
	Weighted k-NN	100	100
Ensemble learner	Bagged Tree	99.2	100
	Subspace Discriminant	91.7	90.3
	Subspace k-NN	99.5	100
	RUSboost Tree	100	99.5

Table 3: Summary of researchers showing the accuracy of detection.

Author/Year	Feature extraction method	Classifier	Sensitivity/Accuracy/Reliability	Database Source	Database Availability	Sound capture source	Location of Sound Capture	Data Pre-processing	Data Quantity and other information
Rizal <i>et al.</i> , (2019) [29]	Multi-distance signal level difference (MSCD)	Multi layer perceptron (MLP)	Acy. 98.99%	RALE [19], Wilkins [30]	CA	CAcc. (EMT25, Siemens)	Chest wall	SF 8 kHz	N=109 HLS 22, A 18, C 20, Fpr 19, So 20
Shi <i>et al.</i> , (2019) [31]	Temporal features Mel spectrogram features	Bi GRU-VGGish	Acy. 87.41%	NM	AWS	3M Littmann 3200 ES	NM	SF 4 kHz	N=384 HLS 120, PS 156, A 108
Niu <i>et al.</i> , (2019) [32]	Time Frequency	Logistic Classifier	Acy. 93.36%	Baidu Cloud repository [33]	CA	Capacitive microphone SKC MP 40	NM	3 rd O Bu. BPF IIR 20-600 Hz	N=220
Shi <i>et al.</i> , (2019) [7]	WCC	BPNN	Acy. 92.5%	NM	AWS	3M Littmann DS	NM	SF 4 kHz	N=64 HLS 6, DR 29, MR 29
Proposed method	Power spectrum and WBS	DT, SVM, k-NN, EL	Acy. 90% to 100%	RALE [19], [20-22]	CA	CAcc. (EMT25, Siemens)	Chest wall	SF 4 kHz, HPF 7.5 kHz, LPF 2.5 kHz, BPF 150 Hz-2 kHz	N= 372 HLS 50, W 252, C 70

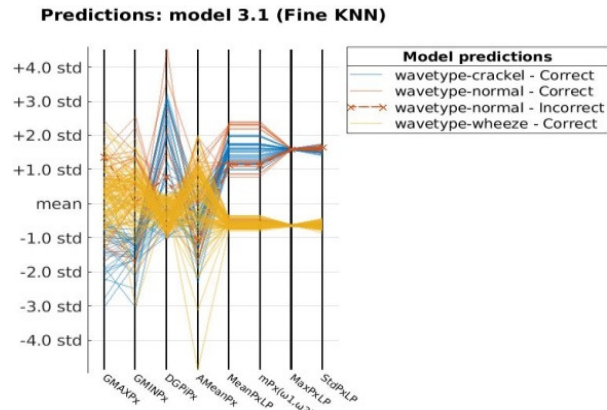


Fig. 11. Parallel coordinates graph of fine k-NN in wavelet bi-spectrum.

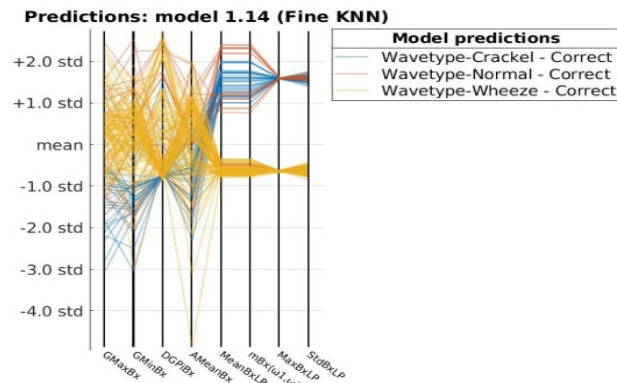


Fig. 12. Parallel coordinates graph of fine k-NN in the power spectrum.

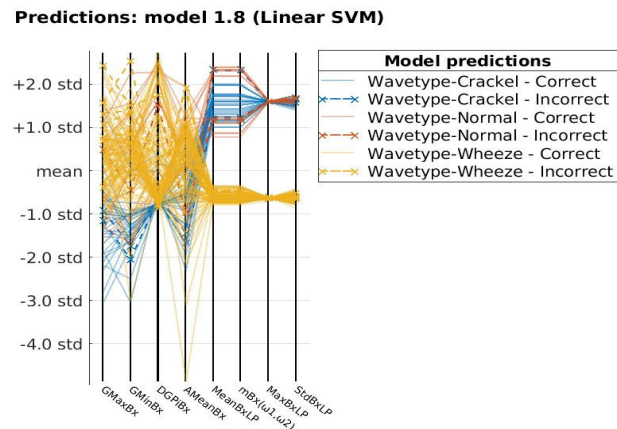


Fig. 13. Parallel coordinates graph of linear SVM in the power spectrum.

The solid lines in the plot mention the median values for each group and the dotted lines as the quartile values of the same color. As an example, in the case of wave type crackle, the solid lines show the median value measured for each variable. The dotted lines above solid lines signify the 75 percent of measurements for each variable, and the dotted lines below show 25 percentage measurements for each variable on wave-type crackle and similarly for wave-type normal sound and wheezes.

VII. CONCLUSION

Adventitious sounds of obstructive pulmonary diseases like Asthma and COPD possess non-stationary nature. The higher-order spectral analysis provides a useful tool for the classification of adventitious sounds like wheezes, crackle, and normal sounds. Sixteen introduced features based on the wavelet bi-spectrum and power spectrum are presented in this research. Some of the feature classifier combinations have yielded 100% accuracy. Average accuracy achieved in the case of wavelet bi-spectrum outperforms that achieved in the case of the power spectrum.

VIII. FUTURE SCOPE

Based on research after a more significant number of trails, the set of features and classifiers can be locked for the real-time classification process. The system with data-collecting sensors, pre-processing data, controllers, and the classification approaches for the real-time identification of adventurous sounds may be of great help for medical research professionals. Also, the combination of feature classifiers can be applied for the classification of any other type of defined sound.

ACKNOWLEDGMENT

Researchers are thankful to Research Center Military College of Telecommunication Engineer (MCTE), MHOW, Ministry of Defense, Government of India, DAVV University and IPS Academy, Institute of Engineering and Science Indore India. The authors are also thankful to SDBCE Indore India.

Conflict of Interest. No conflict of interest to declare.

REFERENCES

- [1]. WHO, M. (2019). *Cronic respiratory diseases*. Retrieved Jan. 23, 2020, from World Health Organisation: <http://www.who.int/respiratory/asthma/en/>
- [2]. Gavriely, N. (1995). *Breath Sound Methodology*. Boca Raton, FL: CRC Press.
- [3]. Murphy, R., Holford, S., & Knowler, W. (1977). Visual Lung Sound Characterization by time expanded wave-form analysis. *New England J. Med.*, 968-971.
- [4]. Shabtai-Musih, Y. A. E. L., Grotberg, J. B., & Gavriely, N. O. A. M. (1992). Spectral content of forced expiratory wheezes during air, He, and SF6 breathing in normal humans. *Journal of Applied Physiology*, 72(2), 629-635.
- [5]. Taplidou, S. A., & Hadjileontiadis, L. J. (2007). Wheeze detection based on time-frequency analysis of breath sounds. *Comput. Biol. Med.*, 37(8), 1073-1083.
- [6]. Dubey, R., & Bodade, R. M. (2019). Classification Techniques Based on Neural Networks for Pulmonary Obstructive Diseases: A Review. *Int. Conf. Recent Adv. in Interdis. Trends in Eng. & Appl. (RAITEA-2019)*, 21-27.
- [7]. Shi, Y., Li, Y., Cai, M., & Zhang, X. D. (2019). A Lung Sound Category Recognition Method Based on Wavelet Decomposition and BP Neural Network. *Int. J. Biological Sci.*, 15, 195-207.
- [8]. Chatterjee, S., & Rahman, M. M. (2019). WheezeD: Respiration Phase Based Wheeze Detection Using Acoustic Data From Pulmonary Patients Under Attack. *13th EAI Int. Conf. on Pervasive Computing Tech. for Healthcare - Demos and Posters*, 1-4.

- [9]. Hadjileontiadis, L. J., & Panas, S. M. (1997). Nonlinear Analysis of Musical Lung Sound Using the Bicoherence Index. *Proc. 19th Annu. IEEE Int. Conf. EMBS*, 3, 1126-1129.
- [10]. Ahlström, C., Hult, P., & Ask, P. (2005). Wheezes Analysis and Detection with Nonlinear Phase Space Embedding. *Proc. IFMBE 13th Nord. Baltimore Conf. (NBC)*, 305-306.
- [11]. Taplidou, S. A., & Hadjileontiadis, L. J. (2007). Nonlinear Analysis of wheezes using Wavelet bicoherence. *Comput. Biology and Med.*, 37(4), 563-570.
- [12]. Nabi, F. G., Sundaraj, K., & Lam, C. K. (2019). Identification of asthma severity levels through wheeze sound characterization and classification using integrated power features. *Biomed. Sig. Process. and Cont.*, 52, 302-311.
- [13]. Taplidou, S. A., & Hadjileontiadis, J. L. (2010). Analysis of Wheezes Using Wavelet Higher-Order Spectral Features. *IEEE Tran. Biomed. Eng.*, 57(7), 1596-1610.
- [14]. Addison, P. S. (2002). *The Illustrated Wavelet Transform Handbook: Introductory Theory and Applications in Science*. Bristol, PA: Institute of Physics (IoP) Publishing.
- [15]. Nikias, C. L., & Athina, P. P. (1993). *Higher-Order Spectral Analysis, A Non-Linear Signal Processing Framework* (2nd ed.). USA: Prentice-Hall, Inc.
- [16]. Jalori, H., Verma, S., & Gwa, A. (2016). Investigation of Non-linear effect in ELF/VLF waves observed by the DEMETER satellite over seismic regions. *Int. J. of Theoretical and Applied Sci.*, 8(1), 74-80.
- [17]. Welch, P. D. (1967). The Use of Fast Fourier Transform for the Estimation of Power Spectra: A Method Based on Time Averaging Over Short, Modified Periodograms. *IEEE Trans. on Audio and Electroacoustics*, AU-15(2), 70-73.
- [29]. Rizal, A., Hidayat, R., & Nugro, A. H. (2019). Comparison of multi-distance signal level difference Hjorth descriptor and its variations for lung sound classifications. *Indonesian Journal of Electrical Engineering and Informatics (IJEEI)*, 7(2), 345-356.
- [30]. Wilkins, R. L., Hodgkin, J. E., & Lopez, B. (2004). *Fundamentals of Lung and Heart sound* (3 ed.). Maryland Heights, Missouri, USA: Mosby.
- [31]. Shi, L., Du, K., Zhang, C., & Ma, H. (2019). Lung Sound Recognition Algorithm Based on VGGish-BiGRU. *IEEE Access*, 7, 139438-139449.
- [18]. Milligen, B. P., Hidalgo, C., & Anchez, E. S. (1995). Nonlinear phenomena and intermittency in plasma turbulence. *Phys. Rev. Lett.*, 74(3), 395-398.
- [19]. Pasternak, H. (2008). (Dept. of Pediatrics and Child Health, University of Manitoba, Winnipeg, Canada) Retrieved Nov. 15, 2019, from R.A.L.E. Lung Sound 3.2: <http://www.rale.ca/Pricing.htm>
- [20]. BSN, M. R. (1997). *Allnurses*. Retrieved April 10, 2020, from Littman: <http://allnurses.com/general-nursing-student/littman-20-examples-525290.html>
- [21]. Huang, G. (2005). *MedEdPortal*. Retrieved April 10, 2020, from *The Journal of Teaching and Learning Resources*: <http://www.mededportal.org/publication/129/>
- [22]. Keroes, J., Lieberman, D., Etickson, B., Wrigley, D., French, W., & O'Brien, T. (2018). *Medical Training and Simulation*. Retrieved April 10, 2020, from Medical Simulation and Training, LLC.: <https://www.practicalclinicalskills.com/auscultation-lesson-description?coursecaseorder=5&courseid=201>
- [23]. Stone, M. (1974). Cross-validatory choice and assessment of statistical predictions. *J. Royal Stat. Soc.*, 2(36), 111-147.
- [24]. Quinlan, J. R. (1986). Induction of Decision Trees. *Machine Learning*, 1, 81-106.
- [25]. Cortes, C. (1995). Support-Vector Networks. *Machine Learning*, 273-297.
- [26]. Joshi, A., & Mehta, D. A. (2017). Comparative Analysis of Various Machine Learning Techniques for Diagnosis of Breast Cancer. *International Journal on Emerging Technologies*, (Special Issue NCETST-2017) 8(1), 522-526.
- [27]. Altman, N. S. (1981). An Introduction to Kernel and Nearest Neighbor Nonparametric Regression. *Annals of Mathematical Statistics*, 25, 1-31.
- [28]. Sood, M. & Jain, S. (2019). Ensemble Classifier Framework for Epileptic Seizure Classification of EEG Signals. *International Journal on Emerging Technologies*, 10(2), 200-206.
- [32]. Niu, J., Cai, M., Shi, Y., Ren, S., Xu, W., Gao, W., & Reinhardt, J. M. (2019). A Novel Method for Automatic Identification of Breathing State. *Scientific reports*, 9(1), 1-13.
- [33]. Baidu Corporation, B. (2018). Retrieved from Baidu cloud disk repository: https://pan.baidu.com/s/1Q2O4XhAO6bODMJxH_rwd2 Q code: umcx

How to cite this article: Dubey, R., Bodade, R. M., and Dubey, D. (2020). Comparative Analysis of Wavelet bi-spectrum and Power Spectrum Features for the Classification of Adventitious Lung Sound. *International Journal on Emerging Technologies*, 11(3): 320-327.